J BONE ONCOL 40 (2023) 100484

Contents lists available at ScienceDirect

Journal of Bone Oncology

journal homepage: www.elsevier.com/locate/jbo

Research Paper

Comprehensive landscape of TGFβ-related signature in osteosarcoma for predicting prognosis, immune characteristics, and therapeutic response

Dong Liu [a,1], Ye Peng [b,1], Xian Li [c,1], Zhijie Zhu [a], Zhenzhou Mi [a], Zhao Zhang [a,*], Hongbin Fan [a,*]

[a] Department of Orthopaedic Surgery, Xi-jing Hospital, The Fourth Military Medical University, Xi'an 710032, China
[b] Department of Orthopaedics, Air Force Medical Center, PLA, Beijing 100142, China
[c] Department of Orthopaedics, Shenzhen University General Hospital, Shenzhen, China

HIGHLIGHTS

- Our study comprehensively investigated the function of TGFβ-related genes in the progression and prognosis of osteosarcoma.
- Our study provided a precise classification of the immune microenvironment and therapeutic response in patients with osteosarcoma by TGFβ risk model.

ARTICLE INFO

Keywords:
Osteosarcoma
TGFβ
Prognostic prediction
Therapy
Nomogram

ABSTRACT

Osteosarcoma (OS) is a highly heterogeneous malignant bone tumor, and its tendency to metastasize leads to a poor prognosis. TGFβ is an important regulator in the tumor microenvironment and is closely associated with the progression of various types of cancer. However, the role of TGFβ-related genes in OS is still unclear. In this study, we identified 82 TGFβ DEGs based on RNA-seq data from the TARGET and GETx databases and classified OS patients into two TGFβ subtypes. The KM curve showed that the Cluster 2 patients had a substantially poorer prognosis than the Cluster 1 patients. Subsequently, a novel TGFβ prognostic signatures (MYC and BMP8B) were developed based on the results of univariate, LASSO, and multifactorial Cox analyses. These signatures showed robust and reliable predictive performance for the prognosis of OS in the training and validation cohorts. To predict the three-year and five-year survival rate of OS, a nomogram that integrated clinical features and risk scores was also developed. The GSEA analysis showed that the different subgroups analyzed had distinct functions, particularly, the low-risk group was associated with high immune activity and a high infiltration abundance of CD8 T cells. Moreover, our results indicated that low-risk cases had higher sensitivity to immunotherapy, while high-risk cases were more sensitive to sorafenib and axitinib. scRNA-Seq analysis further revealed that MYC and BMP8B were strongly expressed mainly in tumor stromal cells. Finally, in this study, we confirmed the expression of MYC and BMP8B by performing qPCR, WB, and IHC analyses. To conclude, we developed and validated a TGFβ-related signature to accurately predict the prognosis of OS. Our findings might contribute to personalized treatment and making better clinical decisions for OS patients.

1. Introduction

Osteosarcoma (OS) is the most common primary malignant bone tumor with high aggressiveness and metastasis, often occurring in children and adolescents [1,2]. Surgical intervention is an essential treatment for patients with OS [3]. With the spread of neoadjuvant chemotherapy options, combination of chemotherapy with surgery has achieved a 5-year survival rate of 70% for patients with OS [4]. However, patients with recurrent or unresectable OS still have poor outcomes even when enrolled in clinical trials, with a 5-year survival rate of only 20% [5]. The high complexity and heterogeneity of the OS genome has halted the development of novel therapeutic strategies over the past decades [6]. Therefore, it is urgent to explore novel biomarkers to target treatment and improve prognosis for OS.

TGFβ is a multifunctional cytokine that regulates cell cycle, cell differentiation, migration, apoptosis, and immune response. It plays an

* Corresponding authors at: Department of Orthopaedic Surgery, Xi-jing Hospital, The Fourth Military Medical University, Xi'an 710032, China.
E-mail addresses: zhangzhao_98@163.com (Z. Zhang), fanhb@fmmu.edu.cn (H. Fan).
[1] These authors contributed equally to this work.

https://doi.org/10.1016/j.jbo.2023.100484
Received 20 March 2023; Received in revised form 6 May 2023; Accepted 9 May 2023
Available online 12 May 2023

important role in cell development and maintaining tissue homeostasis [7,8]. TGFβ signaling has different or even opposite effects under various pathophysiological conditions, especially in tumors [9]. In precancerous cells, TGFβ acts as a tumor suppressor. It maintains genomic stability and prevents tumor progression by inhibiting cell proliferation and promoting apoptosis. However, as tumors progress, tumor cells can adapt to the inhibitory function of TGFβ and utilize the pro-growth feature of TGFβ to undergo malignant phenotype transformation [10,11]. Moreover, the release of TGFβ from tumor cells, stromal cells, and other cells also facilitates angiogenesis, stromal fibrosis and immune escape to mediate tumor invasion and migration through the reshaping of the tumor microenvironment [12]. Several researchers have found that TGFβ is upregulated in several tumors and is correlated with poor prognosis and immune suppression [13,14]. The main cause of the highly aggressive nature of OS is the dysregulation of the bone matrix remodelling [15–17]. TGFβ is an important cytokine involved in tumor progression and is released from the bone matrix when OS cells invade bone tissue [18]. Previous studies have demonstrated TGFβ is associated with metastasis, angiogenesis, and drug resistance in OS. However, the prognosis and immune effects of TGFβ-related genes in OS remain unclear.

Due to the advancements in bioinformatics and next-generation sequencing technologies, exploring and developing novel biomarkers to treat patients with tumors have become highly reliable and feasible [19–21]. Here, we systematically evaluated the expression of TGFβ-related genes in OS and identified TGFβ subtypes. Then, we constructed a TGFβ nomogram to accurately predict the prognostic outcomes of OS. We also assessed the tumor immune microenvironment (TIME) and the therapeutic responses of different TGFβ risk subgroups. Overall, our study identified prognostic indicators in OS and provided new insights into personalized treatment.

2. Materials and methods

2.1. Data extraction and processing

We obtained RNA-seq data and relevant clinical characteristics for 85 OS tissues from the TARGET database. The RNA-seq data of 396 normal musculoskeletal tissues were downloaded from the GTEx database. To eliminate the differences in the data obtained from the GTEx and TCGA databases, the RNA-seq data for the samples were converted to log2 (FPKM value + 1). Using the combat function, we integrated the GTEx and TARGET datasets into the combined dataset to create a training set using the R package "sva". We also obtained data on 223 TGFβ-related genes from previous study [22] (Table S1). The gene expression data and clinical characteristics of 53 OS patients in the GSE21257 from the GEO database were used as the independent validation set. The clinical information for osteosarcoma patients is presented in Table S2.

2.2. Differential expression of TGFβ-related genes and functional enrichment analysis

Using the R package "limma", the TGFβ differential expression genes (DEGs) of OS compared to healthy tissue were analyzed based on the thresholds of |log2(fold change, FC)|>1 and false discovery rate (FDR) < 0.05. Subsequently, the "ClusterProfiler" package of the R software was used for performing the Kyoto Encyclopedia of Genes and Genomes (KEGG) and Gene Ontology (GO) analyses of TGFβ DEGs.

2.3. Consensus clustering

According to the expression matrix of TGFβ DEGs, the R package "ConsensusClusterPlus" was used to recognize TGFβ subtypes for OS patients. The clustering matrix and the cumulative distribution function (CDF) were used to identify the most appropriate cluster count. Then, we performed principal component analysis (PCA) to identify different subtype profiles. The KM curve was used to assess the prognostic characteristics of different subtypes.

2.4. Establishing and verifying the TGFβ signature

First, we conducted univariate regression to screen for prognosis-related TGFβ DEGs in the training cohort. Then, the LASSO regression analysis and the multi-factor Cox analysis were performed to further optimize and develop the TGFβ signature. The TGFβ risk scores of various samples were determined using the formula Risk score = Σin (Coefi*Xi) [23,24]. Then, we used the KM and time-dependent receiver operating characteristic (ROC) curves to evaluate and confirm the reliability of the TGFβsignature for the training and validation cohorts.

2.5. Correlation of TGFβ risk scores with clinical features

We extracted the clinical data (gender, age, and metastatic status) from the training cohort and analyzed their relationship with the TGFβ risk score. Additionally, by integrating the TGFβ risk scores and the clinical features, univariate/multivariate regression was performed to determine the independent predictive ability of the risk scores for OS prognosis.

2.6. Nomogram construction and calibration

We constructed the predictive nomogram for predicting the three-year and five-year survival in patients with OS based on the TGFβ risk scores and the clinicopathological features. We also used ROC curves, calibration plots, and the C-index for weighing the nomogram predicting ability.

2.7. Gene set enrichment analysis (GSEA)

For determining the differences in functions of high-risk and low-risk groups, we performed the GSEA for comparing hallmark gene set enrichment levels of both groups, based on the thresholds of |NES| > 1, FDR < 0.25, and NOM p < 0.05.

2.8. Tumor immune microenvironment (TIME) and drug sensitivity analysis

We used the CIBERSORT algorithm for assessing immune cell infiltration levels within different risk groups. CIBERSORT can be used to evaluate 22 immune cells by deconvolution based on the expression matrix. We also evaluated differences in immune checkpoints (CTLA4, TIGIT, and BTLA) between risk subgroups to predict responses to immunotherapy. Additionally, the half-maximal inhibitory concentrations (IC50) of the targeted drug in different risk subgroups were predicted using the R package "pRRophetic" [25].

2.9. scRNA-Seq data processing and analysis

The scRNA-Seq of GSE162454 obtained from GEO database, including 6 primary osteosarcoma samples. The R package "Seurat" was then used to preprocess standardized scRNA-Seq data. To obtain high-quality single-cell data, we filtered for genes expressed in fewer than three cells, as well as for cells with<200 or>6000 genes detected, in addition to those with high mitochondrial content (>15%). After discarding the poor quality cells, a total of 48,484 cells were retained for downstream analysis. The scRNA-seq data were normalized using LogNormalize before removing batch effects, PCA, and Uniform Manifold Approximation and Projection (UMAP) dimensionality reduction. The "FindClusters" function in the R package "Seurat" was used to perform cell clustering and R package "SingerR" was used to annotate cell subpopulations. The "FindALLMarkers" function was used to determine the

DEGs between subpopulations, with $\log_2|FC| > 0.5$ & pvalue < 0.05 set as thresholds.

2.10. Cell culture

The OS cells (HOS, MG-63) and hFOB 1.19 osteoblasts were purchased from Procell Life Science Technology Co., Ltd. All cells were cultured in DMEM, including 1% P/S (Solarbio, China) and 10% fetal bovine serum (FBS, Gibco, USA), followed by incubation at 37 °C and 5% CO_2.

2.11. Western blot (WB) assay

The RIPA lysis buffer (Beyotime, China) was used for extracting proteins from cells. We used a BCA protein assay kit (Solarbio, China) for quantifying proteins. The proteins were then boiled, loaded, separated by electrophoresis, and transferred onto NC membranes. Using suitable primary antibodies, including anti-MYC(1:5000, 67447–1-Ig, Proteintech, China), anti-BMP8B(1:1000, bs-3670R, Bioss, China), and anti-GAPDH (1:5000, 60004–1-Ig, Proteintech, China), the cell membranes were blocked with skim milk and incubated under 4 °C overnight, followed by incubation with the secondary antibody (1:2,000) for 1 h at room temperature and observation by ECL luminescence.

2.12. Quantitative polymerase chain reaction (qPCR)

For extracting total cellular RNA, the TRIzol method was used. For the reverse transcription of RNA, a cDNA synthesis kit (Takara, China) was used. The Bio-Rad CFX96 Real-Time PCR system (Bio-Rad, USA) was used for performing qRT-PCR by using TB Green Premix ExTaq II (Tli RNaseH Plus). GAPDH was used as the internal control. The primer sequences used for performing the PCR are shown in Table 1. The assay was repeated in triplicate.

2.13. Immunohistochemistry (IHC)

In total, 10 pairs of paraffin-embedded OS tissues and adjacent tissues were collected for further validation of the expression of the candidate gene by immunohistochemical analysis. This study was approved by the Institutional Review Board of Xijing Hospital, Fourth Military Medical University. The participants all provided informed consent. All tissue sections were dewaxed, fixed with an antigen, blocked, and incubated with primary and secondary antibodies (MYC,1:500; BMP8B,1:200). Finally, the DAB kit (CWBIO, CW2035S) was used for color rendering and hematoxylin re-staining. The sections were examined under a microscope, and the positive rate of each immunohistochemically stained section was calculated using the Image J software.

2.14. Statistics

Statistical analysis was conducted using the R 4.0.5 software, SPSS 21.0, and GraphPad Prism 8. We performed t-tests to determine differences between experimental groups and performed a one-way ANOVA to determine differences among the three groups. All differences among and between groups were considered to be statistically significant at $P < 0.05$ (*$p < 0.05$, **$p < 0.01$, and ***$p < 0.001$).

Table 1
The primer sequences of the candidate genes.

Gene	Sequence (5′ -> 3′)
BMP8B	Forward: AAGGCCTAGATGTCTTGCGG Reverse: GACTCTTCTTGTTTCTGTGCCG
MYC	Forward: TTACAACACCCGAGCAAGGA Reverse: AAATACGGCTGCACCGAGTC
GAPDH	Forward:GGAGCGAGATCCCTCCAAAAT Reverse:GGCTGTTGTCATACTTCTCATGG

3. Results

3.1. Determination of TGFβ DEGs and functional annotation

The flow chart of this study is shown in Fig. 1. In total, 82 TGFβ DEGs were detected between OS tissues and normal tissue, of which 48 TGFβ genes were upregulated, and 34 were downregulated (Fig. 2A-B). Then, functional enrichment of these DEGs was performed, and the results of the KEGG analysis showed that these DEGs were associated with the TGFβ signaling pathway, Hippo signaling pathway, Human papillomavirus infection, and etc., (Fig. 2C). The results of the GO analysis showed that these DEGs were mostly involved in Transmemebrance protein serine/threonine kinase signaling pathway, Transforming growth factor beta receptor, Response to growth factor, and etc., (Fig. 2D).

3.2. Classification of the TGFβ subtypes by cluster analysis

Based on the expression profiles of the DEGs, we identified two TGFβ subtypes for patients with OS (Fig. 3A-B). The results of the PCA analysis showed that these subtypes could be distinguished (Fig. 3C). Sankey diagrams were used to demonstrate the clinical features in the different subtypes (Fig. 3D). Additionally, as revealed by the results of the KM curve analysis, Cluster 2 patients showed considerably shorter survival time than Cluster 1 patients, suggesting that TGFβ subtypes could affect the prognosis of patients with OS (Fig. 3E).

4. Construction and validation of a TGFβ prognostic signature for OS

Based on the results of univariate regression, we found 12 TGFβ DEGs associated with OS prognosis, with nine genes were risk factors and three genes were protective factors (Fig. 4A). The results of the LASSO regression and the multivariate Cox regression were used to further filter the most significant candidate genes and construct a prognostic signature for patients with OS (Fig. 4B-C). We detected two genes for constructing a TGFβ signature to predict the prognosis of OS. The risk score was calculated as follows: Risk score $= 0.548 \times$ BMP8B $+ 0.822 \times$ MYC. We then divided the training cohort into two groups based on the risk score. The risk score distribution, survival status, and heat map for the candidate gene expression patterns are shown in Fig. 5A-B. We found that with an increase in the risk score, the patient survival in the training set decreased significantly. The KM curve showed that the high-risk cases had a considerably poorer prognosis than the low-risk cases (Fig. 5C). Additionally, the AUC values for the one-year, three-year, and five-year ROC curves were 0.927, 0.792, and 0.814, respectively, suggesting that the TGFβ signature had high accuracy (Fig. 5D). Additionally, we evaluated the prognostic signature in the validation cohort and obtained results similar to that of the training cohort (Fig. 5E-F). The high-risk cases were associated with a considerably poorer prognosis than the low-risk cases (Fig. 5G). The one-year, three-year, and five-year AUC values were 0.735, 0.776, and 0.714, respectively (Fig. 5H). These results showed that the TGFβsignature was accurate and reliable for predicting OS prognosis.

4.1. Relationship between the TGFβ risk score and the clinicopathological characteristics of OS

We further evaluated the association between the TGFβ risk score and the clinicopathological features of OS. The results showed that the risk score was not significantly different for gender and age (Fig. 6A-B). We found that the risk scores were strongly associated with OS metastasis (Fig. 6C). Based on the classification of OS metastases, the TGFβ risk score predicted the prognostic outcome of OS (Fig. 6D-E). The

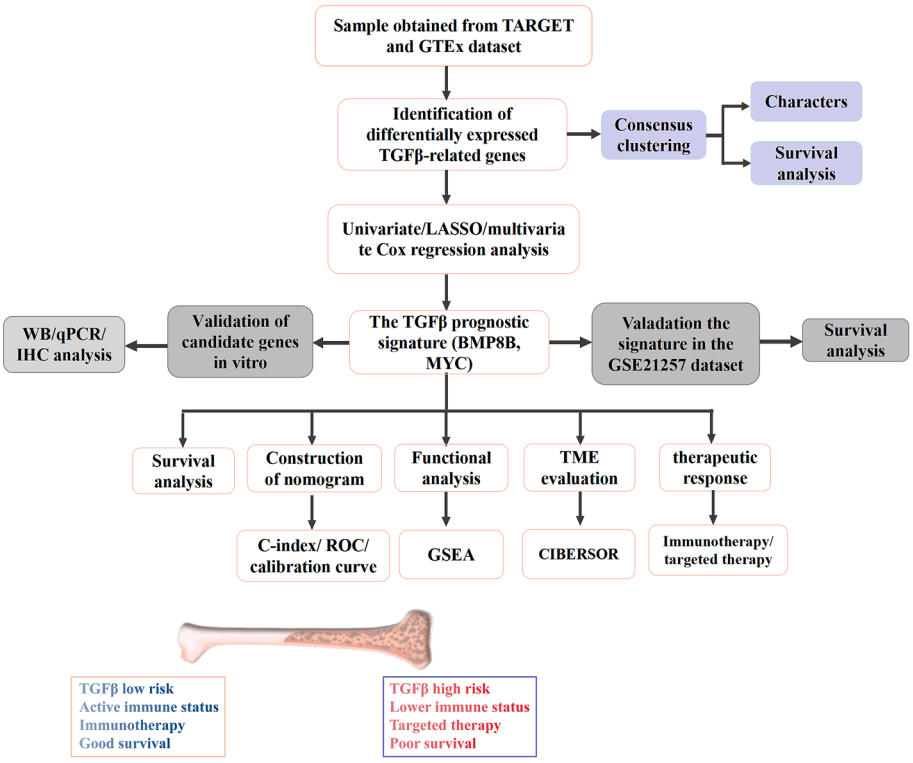

Fig. 1. The flow chart of this study.

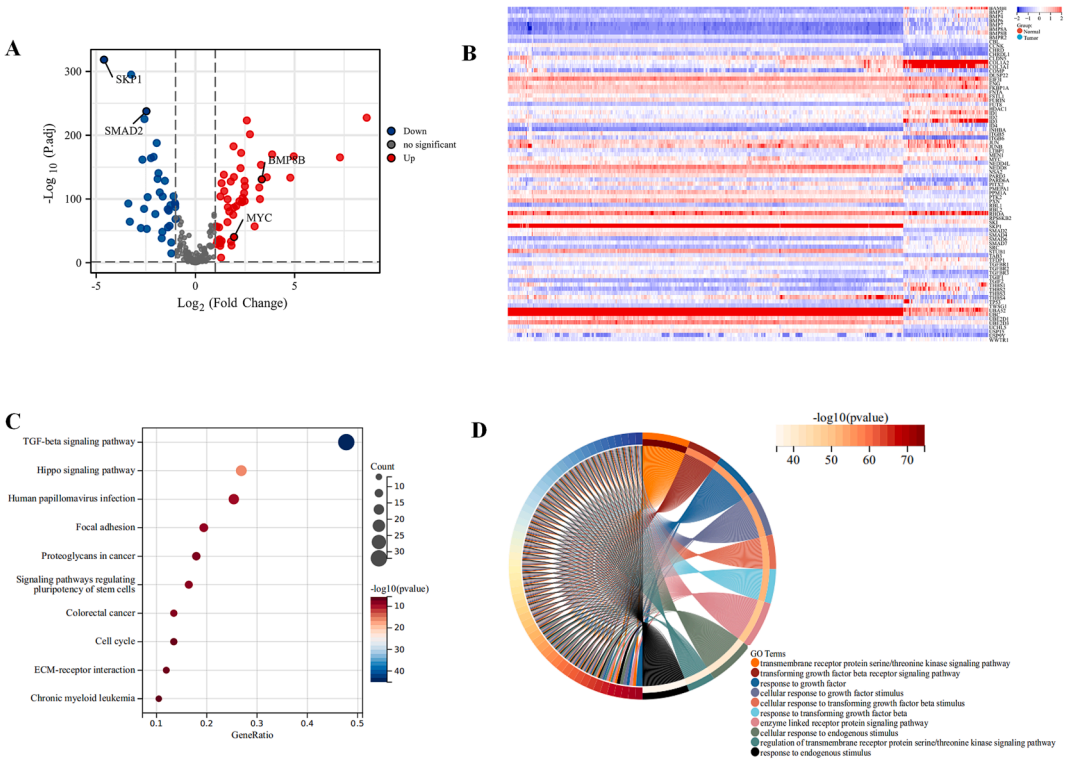

Fig. 2. Identification of TGFβ DEGs between OS and normal tissues. (A). Volcano plot of TGFβ-related gene expression; (B). Heat map of TGFβ DEGs; (C-D). KEGG and GO enrichment analysis of DEGs.

results of the univariate/multivariate regression revealed the independent predictive ability of the TGFβ risk score in OS (Fig. 6F-G).

4.2. Construction of a nomogram

A nomogram was constructed with gender, age, tumor site, metastases, and risk scores to predict the three-year and five-year OS

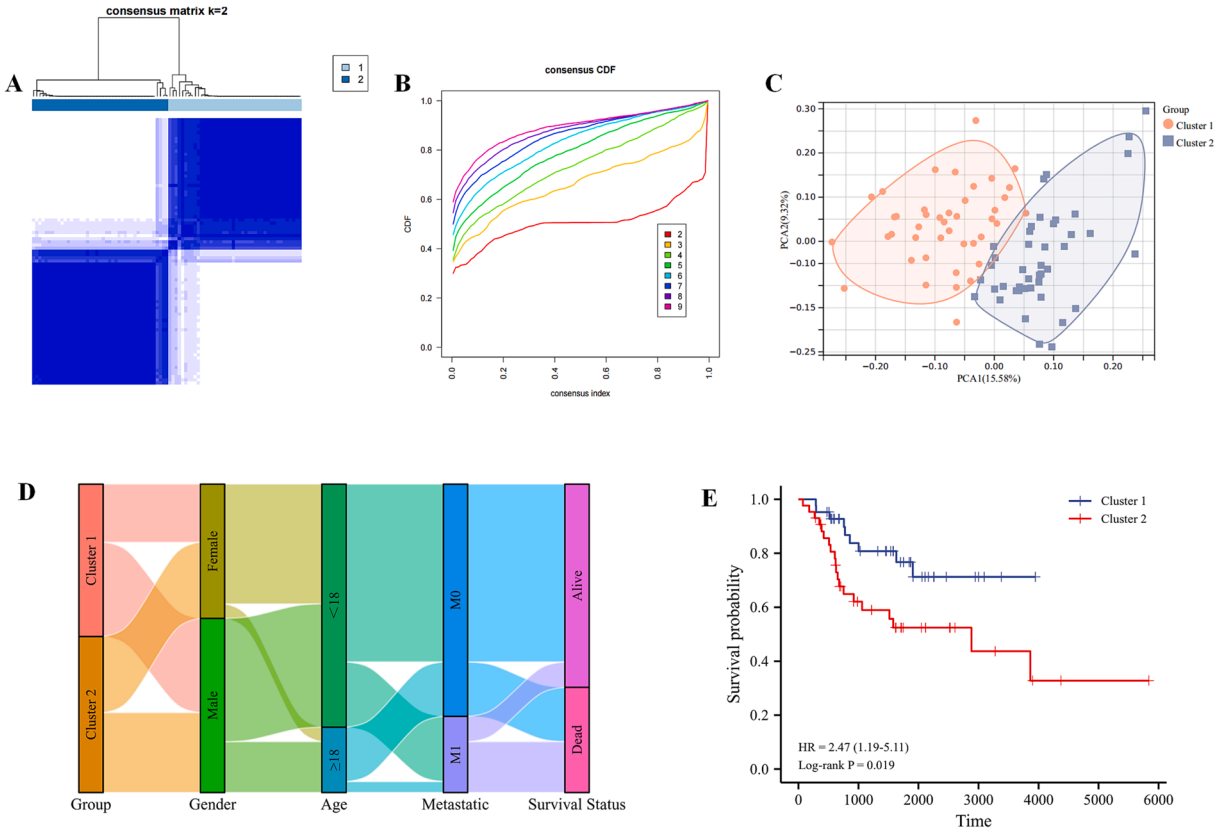

Fig. 3. Recognition of TGFβ subtypes in patients with OS. (A-B). Consensus clustering of OS patients for k = 2; (C). PCA analysis of two different TGFβ subtypes; (D). Sankey diagram showing the distribution of TGFβ subtypes with clinical features; (E). Prognostic analysis of different TGFβ subtypes.

A

Genes	HR(hazard ratio)	HR 95%CI(lower)	HR 95%CI(upper)	p-value
BAMBI	1.29	1.06	1.58	0.012
BMP8A	1.53	1.21	1.95	<0.001
BMP8B	1.43	1.16	1.77	0.001
CBL	1.96	1.1	3.49	0.022
ENG	0.62	0.41	0.96	0.031
FURIN	1.7	1.1	2.61	0.018
ID2	1.61	1.03	2.53	0.037
MYC	1.88	0.32	2.68	<0.001
PMEPA1	0.69	0.52	0.91	0.009
PXN	0.43	0.24	0.76	0.004
SMAD6	1.31	1	1.73	0.047
SMAD7	1.54	1.04	2.29	0.029

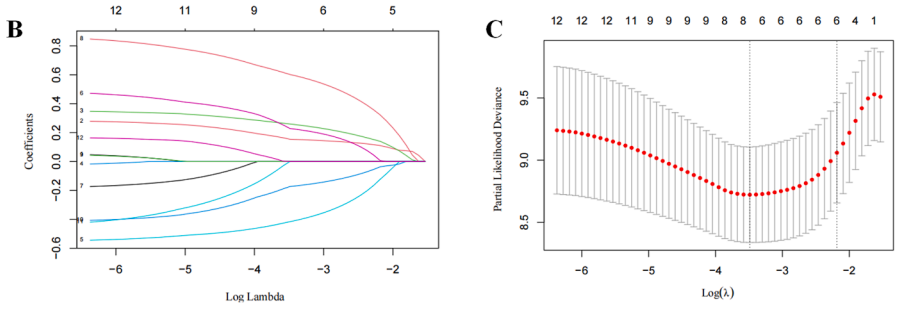

Fig. 4. The establishment of the TGFβ-related prognosis signature. (A). Forest plot showing prognosis-related TGFβ DEGs in the training; (B-C). Optimization of candidate genes by LASSO model with the minimal lambo value.

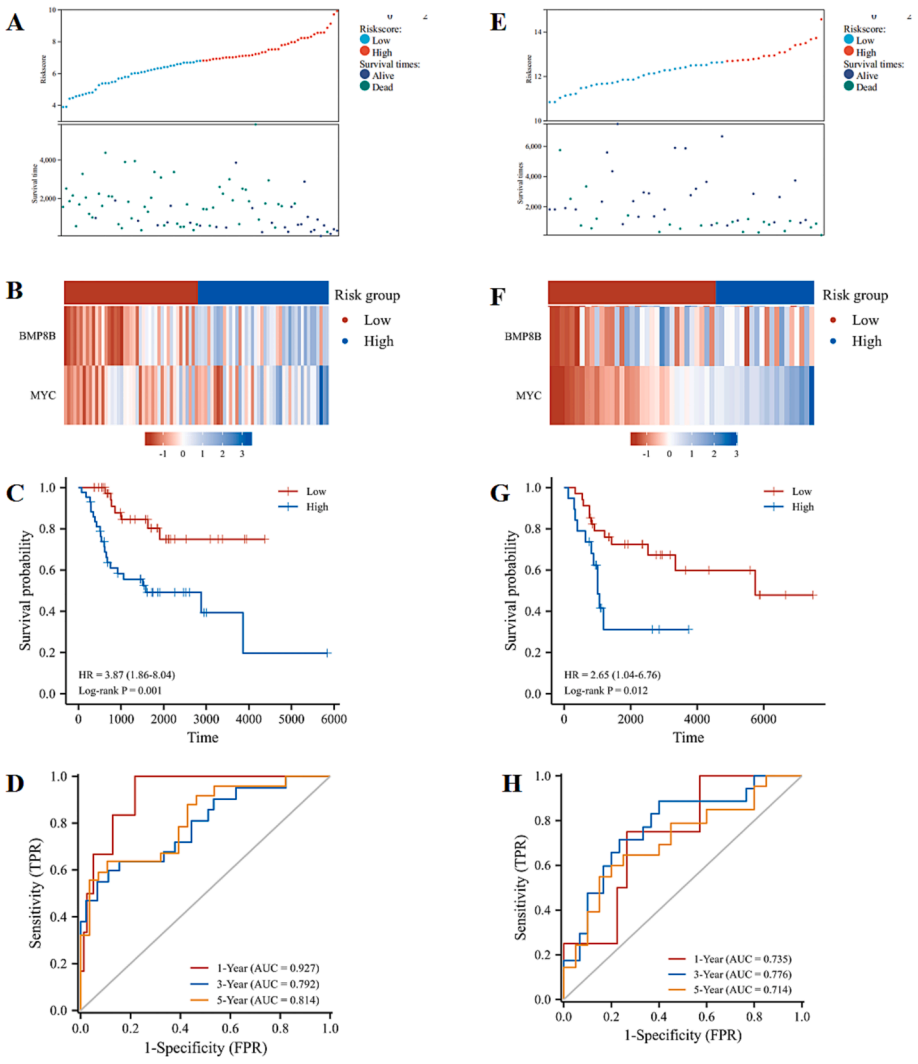

Fig. 5. Evaluation and validation TGFβ-related signature. Distribution plots of the risk score and survival status in the training (A) and validation cohort (E); Heat map demonstrating the expression of candidate genes in the training (B) and validation cohort (F); The survival analysis in the training (C) and validation cohort (G); The ROC curve for the training (D) and validation cohort (H).

prognostic outcome for the training set (Fig. 7A). The C-index of nomogram was found to be 0.875. As indicated by the calibration plot, our nomogram signature performed similarly to the ideal signature (Fig. 7B-D). We also determined the ROC curves for the constructed signature, and the three, five and seven-year AUCs were 0.883,0.909 and 0.841, respectively (Fig. 7E).

4.3. GSEA analysis for different risk subgroups

GSEA was conducted for different TGFβ risk subgroups to determine potential hallmarks affecting OS prognosis. Our results showed that oxidative phosphorylation, MYC target V1, and E2F target functions increased considerably among high-risk cases relative to low-risk cases, whereas Interferon γ response, Inflammatory response, and IL6/JAK/STAT3 functions increased considerably among low-risk patients (Fig. 8A-B). These findings indicated that there were different biological functions in both groups.

4.4. Evaluation of the tumor immune microenvironment and the therapeutic response

Considering the important functions of the immune microenvironment in the prognosis of OS, we performed an immune assessment of patients with different risk subtypes. The results showed that T follicular helper cells and CD8 T cells increased considerably in infiltration abundance among low-risk patients, while gamma-delta T cells and resting dendritic cells showed the opposite results (Fig. 9A). Moreover, the expression of immune checkpoints CTLA4, TIGHT, and BTLA increased considerably among low-risk patients relative to high-risk patients, suggesting that low-risk cases might be the candidates for immunoblocking therapy (Fig. 9B-D). The results of a drug sensitivity analysis showed significantly lower IC50 values for sorafenib and axitinib among high-risk cases relative to that among low-risk cases (Fig. 9E-F).

4.5. ScRNA-Seq analysis of candidate genes in OS

After cell quality control, a total of 48,484 cells were identified in 6 osteosarcoma scRNA-Seq samples (Figure S1). Fourteen distinct clusters were identified after PCA and UMAP analysis (Fig. 10A). Then, a total of nine cell types were discovered by annotation of subpopulations with SingerR and cell-specific marker genes (Fig. 10B). Heat map showing the top 10 marker genes for different cell types (Fig. 10C). We found that MYC was highly expressed in osteoblasts, mesenchymal stem cells (MSC) and cancer-associated fibroblasts (CAF), and BMP8B was highly expressed in CAFs. Figure S2 present the distribution of candidate genes

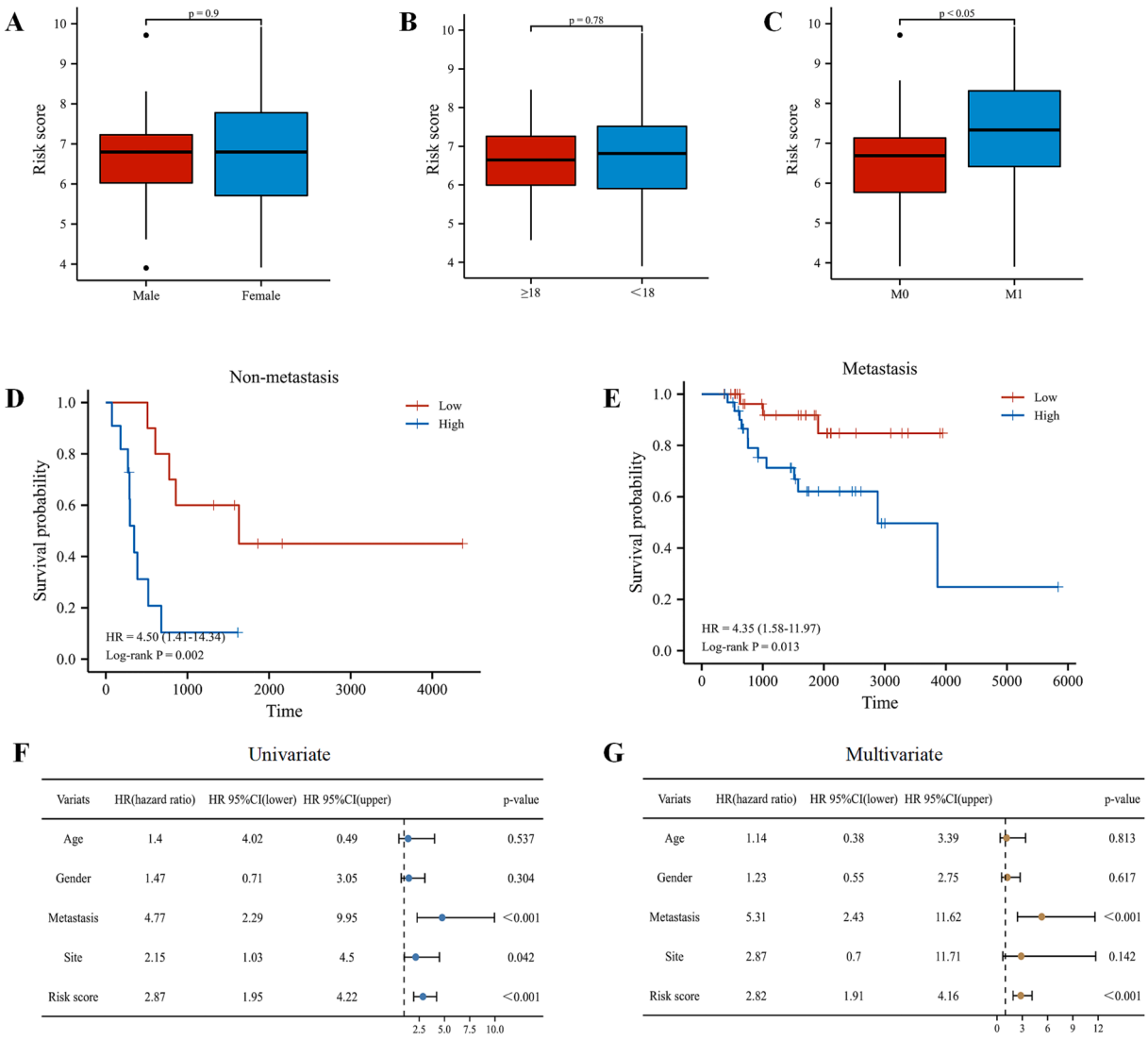

Fig. 6. Relationship between TGFβ risk scores and clinical characteristics. (A). Differences in risk scores of patients with OS with regard to age, sex, and metastatic status; (B-C). Survival analysis of patients with OS regrouped according to metastatic status; (D-E). Univariate and multivariate Cox regression analysis tested the prognostic role of TGFβ risk score and clinical characteristics. *p < 0.05, **p < 0.01, and ***p < 0.001.

in different cell subpopulations.

4.6. *In vitro validation of candidate genes by qPCR, WB, and IHC*

We further determined the gene expression in OS cells and healthy controls by conducting experiments. We found that MYC and BMP8B levels increased considerably in OS cells compared to their levels in normal cells (Fig. 11A-C). Their expression also increased substantially in OS tissues relative to their expression in paracancerous tissues (Fig. 11D-G). These findings were similar to the results of the bioinformatic analysis, thus, increasing the reliability of our study.

5. Discussion

In this study, we identified 83 TGFβ DEGs between OS tissue and normal control tissue. Following functional enrichment of these DEGs, two TGFβ subtypes with distinct prognostic characteristics were identified by performing cluster analysis. We screened the two most important candidate genes (MYC and BMP8B) by univariate/lasso/multivariate analyses and constructed a TGFβ prognostic signature. The ROC and KM curves showed that the TGFβ prognosis nomogram exhibited excellent predictive capability for OS prognosis for the training and validation cohorts. Moreover, we assessed functional variance and the TIME features in both risk groups. The patients in the low-risk group had a higher immune function and immune cell infiltration relative to those in the high-risk group. Finally, scRNA-Seq analysis revealed that MYC and BMP8B were highly expressed in stromal cells, suggesting that TGFβ might exert pro-tumor effects through regulating the communication between tumor stroma and malignant cells. These findings provided a novel perspective for personalized treatment, as well as prognosis prediction of OS.

TGFβ prognostic signature was composed of two genes, MYC and BMP8B, both of which were risk factors for the prognosis of osteosarcoma. MYC has been shown to be an essential proto-oncogene with a role in cell cycle progression, apoptosis and cell transformation [26]. In normal cells, TGFβ signaling can inhibit cell proliferation through blocking the transcription of MYC proto-oncogene. While when MYC mutation occurred, it antagonized TGFβ-induced suppressive effect by regulating the expression of cell cycle transcription factors, thus leading to the proliferation of tumor cells [27,28]. Research has demonstrated that upregulation of MYC in osteosarcoma cells may be critical in counteracting TGFβ growth inhibitory signaling to regulate cell cycle progression [29]. Han et al. found that overexpression of MYC might facilitate the invasion of osteosarcoma cells via activating MEK-ERK

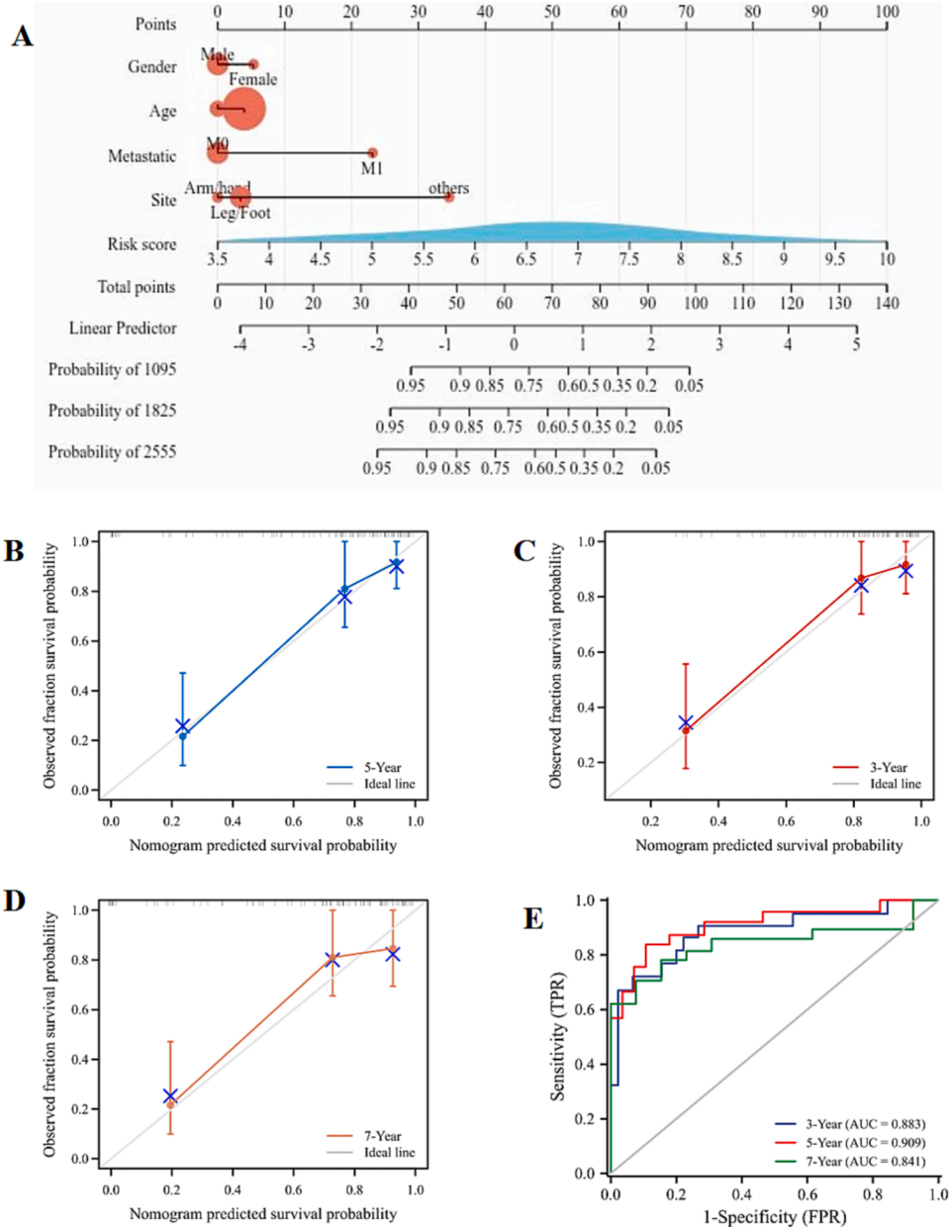

Fig. 7. Establishment of a predictive nomogram. (A). The nomogram based on TGFβ risk score and clinical characteristics to predict the prognosis at 3, 5, and 7 years; (B-D). The calibration curves of the nomogram in 1, 3 and 5-year, respectively; (E). The ROC curves of the nomogram.

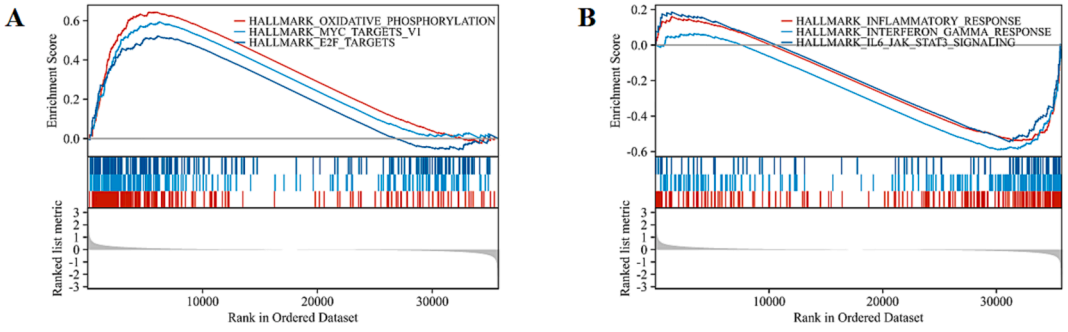

Fig. 8. Gene set enrichment analysis between the different TGFβ risk subgroups (A-B).

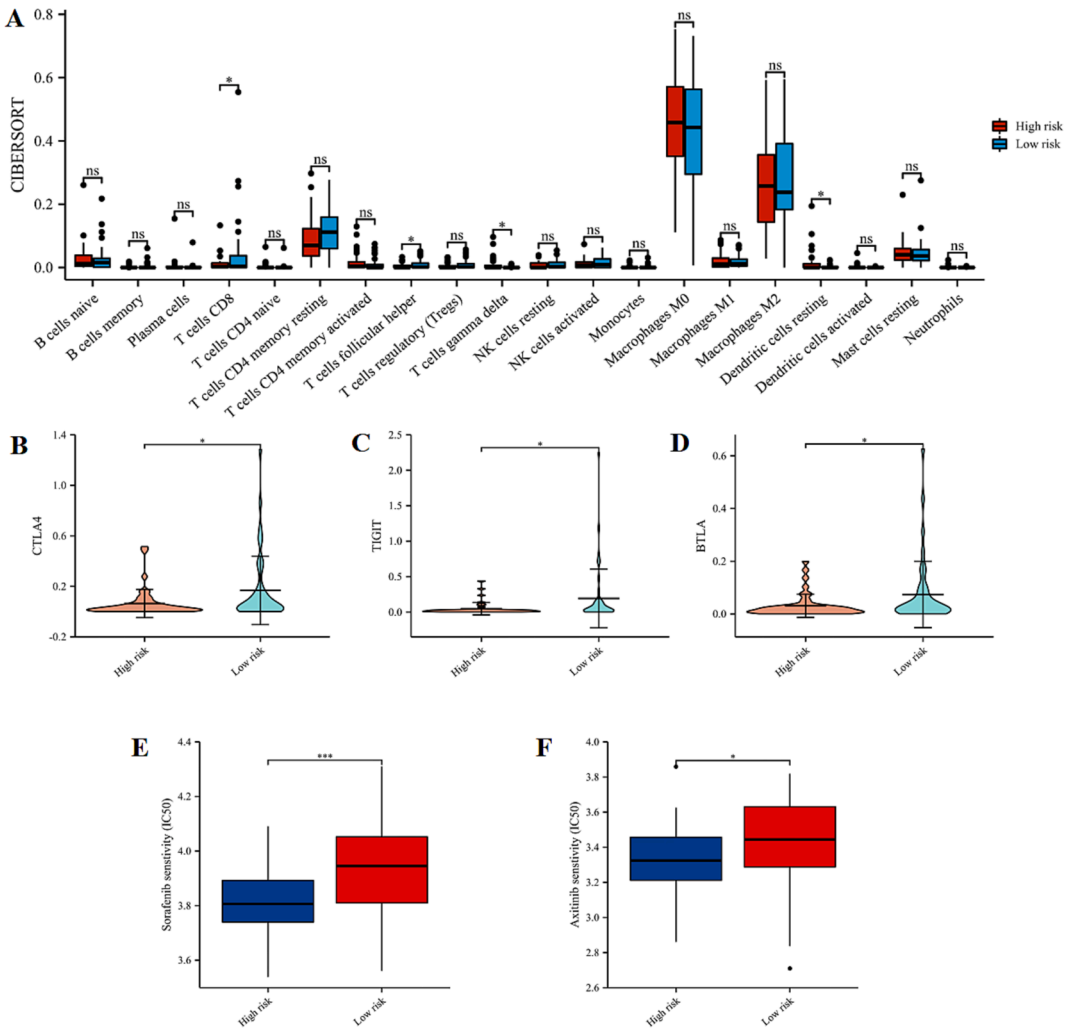

Fig. 9. TIME analysis and therapeutic response in different TGFβ risk subgroups. (A). Differences in the abundance of 22 immune cell infiltrates in different risk subgroups; (B-D). Differential expression of immune checkpoints in different risk subgroups; (E-F). IC50 values for the targeted drugs (sorafenib and axitinib) in different risk subgroups. *p < 0.05, **p < 0.01, and ***p < 0.001.

pathway [30]. In addition, previous studies established that MYC can drive super-enhancer signaling to promote osteosarcoma progression and metastasis [31]. BMP8B, a member of the TGFβ superfamily of proteins, can regulate signaling by binding to various TGFβ receptors, resulting in the recruitment and activation of SMAD family transcription factors. BMP8B is able to bind SMAD2 / 3 and SMAD1 / 5 / 9 transduction signals through the TGFβ-BMP pathway, thereby contributing to inflammation and affecting wound healing [32]. Mima et al. identified that BMP8B upregulation could promote gastric cancer metastasis by modulating the bone marrow microenvironment and was strictly associated with poor prognosis [33]. Cheng et al. found that BMP8B mediated the survivability and invasion of pancreatic cancer cells by modulating the activation of caspase 3/9 [34]. Although the specific mechanism of BMP8B in osteosarcoma is less clear, extensive studies have confirmed that the BMP family was intimately involved in the invasion and metastasis of osteosarcoma [35]. Our study identified that MYC and BMP8B were expressed at high level in osteosarcoma tissues and closely associated with poor prognosis. These results provided new ideas for targeted therapeutic and prognostic markers in osteosarcoma.

TGFβ has been shown to play a dual role in tumor initiation [10]. During early tumor development, TGFβ can promote cell apoptosis and immune surveillance to inhibit tumor proliferation. When the secretion of TGFβ increases, it can reshape the tumor microenvironment to mediate immune escape and tumor invasion [11,12]. Our study revealed that patients in the high-risk group showed remarkably increased tumor progression-related pathways. Notably, immune-related functions were clearly upregulated in the low-risk group. These findings suggested that patients in the high-risk group might be linked to enhanced TGFβ signaling to promote tumor proliferation and progression by regulating the cell cycle, whereas patients in the low-risk group might be able to kill tumor cells by activating adaptive immunity through appropriate TGFβ signaling. Further immune analysis suggested that CD8 T cell infiltration increased considerably in the low-risk group, while the resting dendritic cells showed the opposite pattern. Several studies have shown that TGFβ is a major regulator of the TIME, and its accumulation in the tumor microenvironment can enhance the accumulation of immunosuppressive cell subsets and induce apoptosis of CD8 T cells to inhibit the immune response [36]. CD8 T cells play a key role in the anti-tumor immune response and can specifically recognize tumor-associated antigens to selectively kill tumors. While resting dendritic cell was found to induce CD8 T cell immune tolerance by antigen presentation [37]. Besides, we found that TGFβ candidate genes were highly expressed in CAFs and MSCs, respectively. CAFs and MSCs are essential components of the tumor stroma. TGF-β activation can promote the differentiation of fibroblasts and MSCs to CAFs to mediate the fibrotic remodeling of extracellular matrix [38,39]. Also, CAFs and MSCs can secrete different cytokines to inhibit immune cell activation and infiltration while promoting tumor invasion and metastasis. Thus, we speculated that the

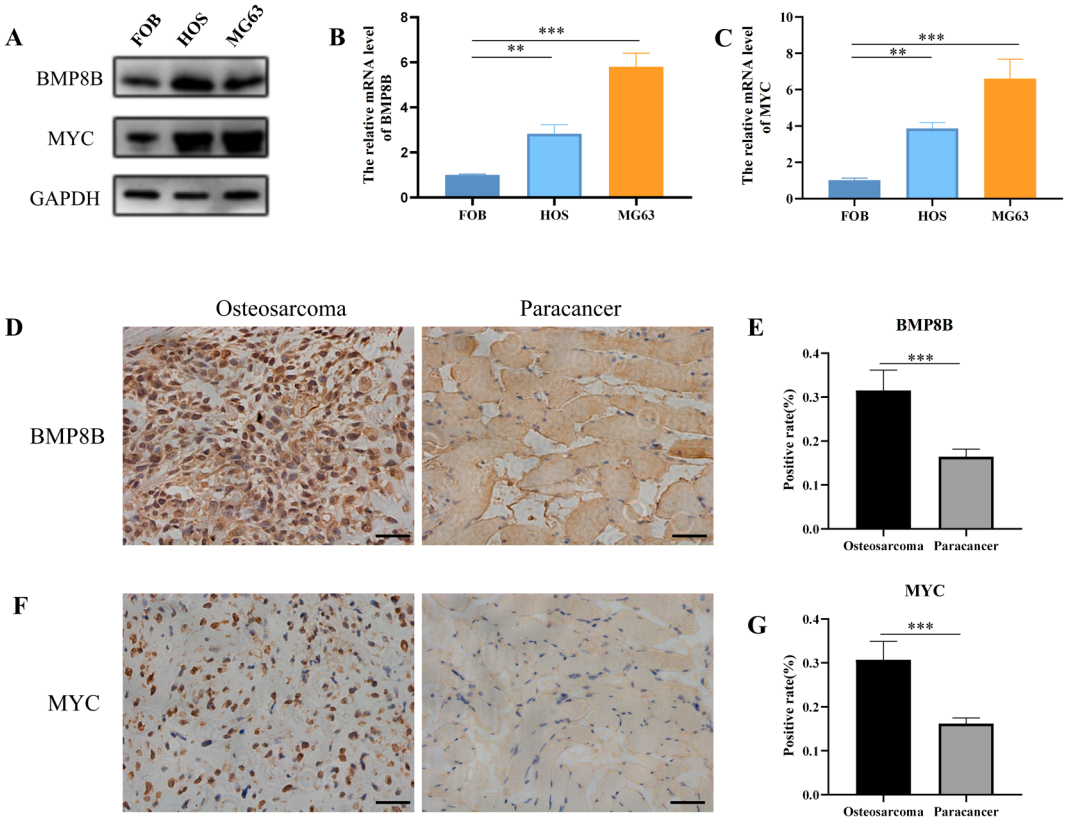

Fig. 10. ScRNA-Seq analysis of candidate genes in OS. (A).UMAP plot showing 48,484 cells from 6 samples; (B).The cell types identified by R package "SingerR"; (C) Heatmap showing the top 10 marker genes in each cell cluster; (D-E) Bubble and violin plots showing the expression levels of candidate genes in different cell types.

TGFβ high-risk group might promote tumor stromal remodeling form an immunosuppressive microenvironment, thereby promoting the metastasis and poor prognosis of OS patients.

Conventional chemotherapy protocols improve the prognosis of most patients with osteosarcoma, however, there are still some patients who lack sensitivity to chemotherapy. Our results revealed that low risk patients showed higher sensitivity to immunotherapy, while high-risk patients might be better adapted to targeted therapy (sorafenib and axitinib). In OS, the tumor stromal has abundant blood flow, and its invasion and metastasis rely on the formation of tumor neovascularization [40]. Sorafenib and axitinib, as tyrosine kinase inhibitors(TKI), can effectively target angiogenic signals and exert antiangiogenic effects, thus inhibiting the malignant behavior of OS [41,42]. Sorafenib was the first targeted therapy shown to be effective in patients with OS. It can significantly prolong survival in patients with recurrent or unresectable OS [43]. Currently, accumulating evidence indicates that TGFβ activation is responsible for upregulating the expression of various receptor tyrosine kinases (RTK), including epidermal growth factor receptor (EGFR), fibroblast growth factor receptor (FGFR) and vascular endothelial growth factor receptor (VEGFR) [44,45]. The interaction between TGF-β signaling pathway and RTK pathway can accelerate tumorigenesis and metastasis, thus the clinical management of TKI in patients with TGF-β high risk might be effectively improve the prognosis of patients. Whereas the high expression of immune checkpoints such as CTLA4 in the low-risk group implied that immunotherapy could block these immunosuppressive receptors and increase the immune activity of CD 8 T cells, resulting in enhanced antitumor immunity. We argued that classifying patients with OS based on TGFβ risk scores to tailor therapy might improve the prognosis in clinical decision making. Taken together, these results provided novel insights into the personalized treatment of OS.

There are several limitations of our study. First, this study was based on results from publicly available databases, requiring further validation in large samples. Second, the specific mechanism by which TGFβ influences the prognosis of osteosarcoma, especially its relationship with TIME, still needs further experimental investigation in the future.

6. Conclusion

To summarize, we systematically evaluated the role of TGFβ-related genes in the progression and prognosis of OS. We also developed novel prognostic signatures that could accurately predict the prognosis and might improve the personalized treatment of patients with OS.

7. Ethics statement

The studies involving human participants were reviewed and approved by the Ethics Committee of Xi-Jing Hospital, Fourth Military Medical University. The patients/participants provided their written informed consent to participate in this study.

Funding

This work was supported by National Natural Science Foundation of China(No. 31971272), Sanming Project of Medicine in Shenzhen (No. SZSM201911011) and Xi-jing Hospital Discipline Promotion Program (XJZT21CM).

Declaration of Competing Interest

The authors declare that they have no known competing financial interests or personal relationships that could have appeared to influence the work reported in this paper.

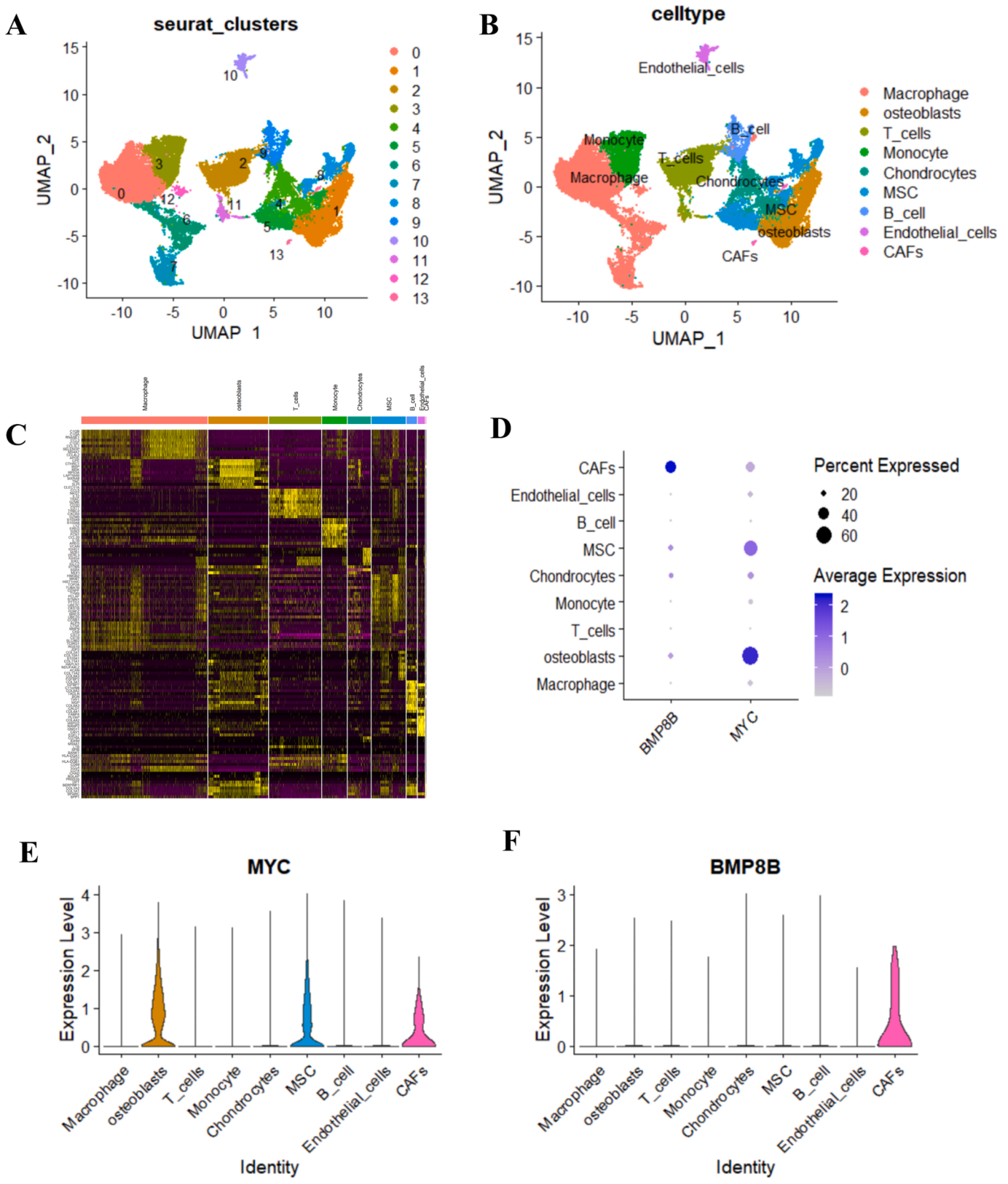

Fig. 11. Validation of candidate genes by WB, qPCR and IHC. (A-C) The expression levels of candidate genes in different cell lines by WB and qPCR; (D-G). The expression levels of candidate genes in OS and paracancerous tissue by IHC, bar = 100um. *p < 0.05, **p < 0.01, and ***p < 0.001.

Data availability statement

Publicly available datasets were analyzed in this study. The datasets used and analyzed in the study are available from the corresponding author on reasonable request.

Appendix A. Supplementary data

Supplementary data to this article can be found online at https://doi.org/10.1016/j.jbo.2023.100484.

References

[1] L. Mirabello, R.J. Troisi, S.A. Savage, Osteosarcoma incidence and survival rates from 1973 to 2004: data from the Surveillance, Epidemiology, and End Results Program, Cancer 115 (2009) 1531–1543, https://doi.org/10.1002/cncr.24121.

[2] Z. Nie, H. Peng, Osteosarcoma in patients below 25 years of age: An observational study of incidence, metastasis, treatment and outcomes, Oncol. Lett. 16 (2018) 6502–6514, https://doi.org/10.3892/ol.2018.9453.

[3] Z. Zhang, Y. Shi, J. Fu, D. Liu, D. Zhu, X. Liu, J. Dang, H. Fan, Customized three dimensional printed prosthesis as a novel intercalary reconstruction for resection of extremity bone tumours: a retrospective cohort study, Int. Orthop. 46 (12) (2022) 2971–2981.

[4] R. Belayneh, M.S. Fourman, S. Bhogal, K.R. Weiss, Update on Osteosarcoma. *Current oncology reports* 23 (2021) 71, https://doi.org/10.1007/s11912-021-01053-7.

[5] J.P. Lagmay, M.D. Krailo, H. Dang, A. Kim, D.S. Hawkins, O. Beaty, 3rd; Widemann, B.C., Zwerdling, T., Bomgaars, L., Langevin, A.M., et al., Outcome of patients with recurrent osteosarcoma enrolled in seven phase II trials through children's cancer group, pediatric oncology group, and children's oncology group: learning from the past to move forward, J. Clin. Oncol. 34 (2016) 3031–3038, https://doi.org/10.1200/jco.2015.65.5381.

[6] Sayles, L.C.; Breese, M.R.; Koehne, A.L.; Leung, S.G.; Lee, A.G.; Liu, H.Y.; Spillinger, A.; Shah, A.T.; Tanasa, B.; Straessler, K.; et al. Genome-Informed Targeted Therapy for Osteosarcoma. *Cancer discovery* 2019, *9*, 46-63, 10.1158/2159-8290.Cd-17-1152.

[7] J. Massagué, TGF-β signaling in development and disease, FEBS Lett. 2012 (1833) 586, https://doi.org/10.1016/j.febslet.2012.05.030.

[8] Y. Zhang, P.B. Alexander, X.-F. Wang, TGF-β family signaling in the control of cell proliferation and survival, Cold Spring Harb. Perspect. Biol. 9 (4) (2017) a022145.

[9] J.F. Santibañez, M. Quintanilla, C. Bernabeu, TGF-β/TGF-β receptor system and its role in physiological and pathological conditions. *Clinical science* 2011 (1979) 233–251.

[10] J.-C. Neel, L. Humbert, J.-J. Lebrun, The dual role of TGFβ in human cancer: From tumor suppression to cancer metastasis, ISRN molecular biology 2012 (2012) 1–28.

[11] P. Papageorgis, T. Stylianopoulos, Role of TGFβ in regulation of the tumor microenvironment and drug delivery (review), Int. J. Oncol. 46 (2015) 933–943, https://doi.org/10.3892/ijo.2015.2816.

[12] J.-F. Chung, M.-K. Chan, J.-F. Li, A.-W. Chan, P.-T. Tang, K.-T. Leung, K.-F. To, H.-Y. Lan, P.-K. Tang, TGF-β signaling: From tissue fibrosis to tumor microenvironment, Int. J. Mol. Sci. 22 (14) (2021) 7575.

[13] X. Jin, S. Zhang, N. Wang, L. Guan, C. Shao, Y. Lin, J. Liu, Y. Li, High expression of TGF-β1 contributes to hepatocellular carcinoma prognosis via regulating tumor immunity, Front. Oncol. 12 (2022), 861601, https://doi.org/10.3389/fonc.2022.861601.

[14] Q. Yu, L. Zhao, X.X. Yan, Y. Li, X.Y. Chen, X.H. Hu, Q. Bu, X.P. Lv, Identification of a TGF-β signaling-related gene signature for prediction of immunotherapy and targeted therapy for lung adenocarcinoma, World J. Surg. Oncol. 20 (2022) 183, https://doi.org/10.1186/s12957-022-02595-1.

[15] Yang, C.; Tian, Y.; Zhao, F.; Chen, Z.; Su, P.; Li, Y.; Qian, A. Bone Microenvironment and Osteosarcoma Metastasis. *International journal of molecular sciences* 2020, *21*, 10.3390/ijms21196985.

[16] J.R. Mortus, Y. Zhang, D.P. Hughes, Developmental pathways hijacked by osteosarcoma, Adv. Exp. Med. Biol. 804 (2014) 93–118, https://doi.org/10.1007/978-3-319-04843-7_5.

[17] K.S. Nørregaard, H.J. Jürgensen, H. Gårdsvoll, L.H. Engelholm, N. Behrendt, K. Søe, Osteosarcoma and metastasis associated bone degradation-A tale of osteoclast and malignant cell cooperativity, Int. J. Mol. Sci. 22 (13) (2021) 6865.

[18] A. Lamora, J. Talbot, M. Mullard, B. Brounais-Le Royer, F. Redini, F. Verrecchia, TGF-β signaling in bone remodeling and osteosarcoma progression, J. Clin. Med. 5 (11) (2016) 96.

[19] Z. Zhang, X. Liu, D. Cheng, J. Dang, Z. Mi, Y. Shi, L. Wang, H. Fan, Unfolded protein response-related signature associates with the immune microenvironment and prognostic prediction in osteosarcoma, Front. Genet. 13 (2022), https://doi.org/10.3389/fgene.2022.911346.

[20] Z. Zhang, Y.e. Peng, J. Dang, X. Liu, D. Zhu, Y. Zhang, Y. Shi, H. Fan, Identification of key biomarkers related to epithelial-mesenchymal transition and immune infiltration in ameloblastoma using integrated bioinformatics analysis, Oral Dis. 29 (4) (2023) 1657–1667.

[21] Z. Zhang, J. Pan, D. Cheng, Y. Shi, L. Wang, Z. Mi, J. Fu, H. Tao, H. Fan, Expression of lactate-related signatures correlates with immunosuppressive microenvironment and prognostic prediction in ewing sarcoma, Front Genet 13 (2022), 965126, https://doi.org/10.3389/fgene.2022.965126.

[22] Z. Liu, T. Qi, X. Li, Y. Yao, B. Othmane, J. Chen, X. Zu, Z. Ou, J. Hu, A novel TGF-β risk score predicts the clinical outcomes and tumour microenvironment phenotypes in bladder cancer, Front. Immunol. 12 (2021), 791924, https://doi.org/10.3389/fimmu.2021.791924.

[23] X. Wang, C. Xie, L. Lin, Development and validation of a cuproptosis-related lncRNA model correlated to the cancer-associated fibroblasts enable the prediction prognosis of patients with osteosarcoma, J. Bone Oncol. 38 (2023), 100463, https://doi.org/10.1016/j.jbo.2022.100463.

[24] Y. Zhang, W. Gan, N. Ru, Z. Xue, W. Chen, Z. Chen, H. Wang, X. Zheng, Comprehensive multi-omics analysis reveals m7G-related signature for evaluating prognosis and immunotherapy efficacy in osteosarcoma, J. Bone Oncol. 40 (2023), 100481, https://doi.org/10.1016/j.jbo.2023.100481.

[25] P. Geeleher, N. Cox, R.S. Huang, J.D. Barbour, pRRophetic: an R package for prediction of clinical chemotherapeutic response from tumor gene expression levels, PLoS One 9 (9) (2014) e107468.

[26] H.L. Moses, TGF-beta regulation of epithelial cell proliferation, Mol. Reprod. Dev 32 (1992) 179–184, https://doi.org/10.1002/mrd.1080320215.

[27] B.K. Law, A. Chytil, N. Dumont, E.G. Hamilton, M.E. Waltner-Law, M.E. Aakre, C. Covington, H.L. Moses, Rapamycin potentiates transforming growth factor beta-induced growth arrest in nontransformed, oncogene-transformed, and human cancer cells, Mol. Cell. Biol. 22 (2002) 8184–8198, https://doi.org/10.1128/mcb.22.23.8184-8198.2002.

[28] Y. Chen, O.I. Olopade, MYC in breast tumor progression, Expert Rev. Anticancer Ther. 8 (2008) 1689–1698, https://doi.org/10.1586/14737140.8.10.1689.

[29] Q. Li, H. Li, X. Zhao, B. Wang, L. Zhang, C. Zhang, F. Zhang, DNA Methylation mediated downregulation of miR-449c controls osteosarcoma cell cycle progression by directly targeting oncogene c-Myc, Int. J. Biol. Sci. 13 (2017) 1038–1050, https://doi.org/10.7150/ijbs.19476.

[30] G. Han, Y. Wang, W. Bi, C-Myc overexpression promotes osteosarcoma cell invasion via activation of MEK-ERK pathway, Oncol. Res. 20 (2012) 149–156, https://doi.org/10.3727/096504012x13522227232237.

[31] D. Chen, Z. Zhao, Z. Huang, D.-C. Chen, X.-X. Zhu, Y.-Z. Wang, Y.-W. Yan, S. Tang, S. Madhavan, W. Ni, Z.-P. Huang, W. Li, W. Ji, H. Shen, S. Lin, Y.-Z. Jiang, Super enhancer inhibitors suppress MYC driven transcriptional amplification and tumor progression in osteosarcoma, Bone Res. 6 (1) (2018), https://doi.org/10.1038/s41413-018-0009-8.

[32] M. Vacca, J. Leslie, S. Virtue, B.Y.H. Lam, O. Govaere, D. Tiniakos, S. Snow, S. Davies, K. Petkevicius, Z. Tong, V. Peirce, M.J. Nielsen, Z. Ament, W. Li, T. Kostrzewski, D.J. Leeming, V. Ratziu, M.E.D. Allison, Q.M. Anstee, J.L. Griffin, F. Oakley, A. Vidal-Puig, Bone morphogenetic protein 8B promotes the progression of non-alcoholic steatohepatitis, Nature metabolism 2 (6) (2020) 514–531.

[33] K. Mima, T. Fukagawa, J. Kurashige, Y. Takano, R. Uchi, H. Ueo, T. Matsumura, M. Ishibashi, G. Sawada, Y. Takahashi, S. Akiyoshi, H. Eguchi, T. Sudo, K. Sugimachi, M. Watanabe, H. Ishii, M. Mori, H. Baba, M. Sasako, K. Mimori, Gene expression of bone morphogenic protein 8B in the primary site, peripheral blood and bone marrow of patients with gastric cancer, Oncol. Lett. 6 (2) (2013) 387–392.

[34] Z. Cheng, W. Cui, Y. Ding, T. Liu, W. Liu, Y. Qin, W. Xia, J. Xu, Y. Zhang, X. Zou, BMP8B mediates the survival of pancreatic cancer cells and regulates the progression of pancreatic cancer, Oncol. Rep. 32 (2014) 1861–1866, https://doi.org/10.3892/or.2014.3413.

[35] A. Nguyen, M.A. Scott, S.M. Dry, A.W. James, Roles of bone morphogenetic protein signaling in osteosarcoma, Int. Orthop. 38 (2014) 2313–2322, https://doi.org/10.1007/s00264-014-2512-x.

[36] B. Chen, C. Mu, Z. Zhang, X. He, X. Liu, The love-hate relationship between TGF-β signaling and the immune system during development and tumorigenesis, Front. Immunol. 13 (2022), 891268, https://doi.org/10.3389/fimmu.2022.891268.

[37] H.C. Probst, K. McCoy, T. Okazaki, T. Honjo, M. van den Broek, Resting dendritic cells induce peripheral CD8+ T cell tolerance through PD-1 and CTLA-4, Nat. Immunol. 6 (2005) 280–286, https://doi.org/10.1038/ni1165.

[38] X. Shi, C.D. Young, H. Zhou, X.-J. Wang, Transforming growth factor-β signaling in fibrotic diseases and cancer-associated fibroblasts, Biomolecules 10 (12) (2020) 1666.

[39] H.X. Tan, Z.B. Cao, T.T. He, T. Huang, C.L. Xiang, Y. Liu, TGFβ1 is essential for MSCs-CAFs differentiation and promotes HCT116 cells migration and invasion via JAK/STAT3 signaling, OncoTargets and therapy 12 (2019) 5323–5334, https://doi.org/10.2147/ott.S178618.

[40] Jiang, Z.Y.; Liu, J.B.; Wang, X.F.; Ma, Y.S.; Fu, D. Current Status and Prospects of Clinical Treatment of Osteosarcoma. *Technology in cancer research & treatment* 2022, *21*, 15330338221124696, 10.1177/15330338221124696.

[41] J.I. Geller, E. Fox, B.K. Turpin, S.L. Goldstein, X. Liu, C.G. Minard, R.A. Kudgus, J. M. Reid, S.L. Berg, B.J. Weigel, A study of axitinib, a VEGF receptor tyrosine kinase inhibitor, in children and adolescents with recurrent or refractory solid tumors: A Children's Oncology Group phase 1 and pilot consortium trial (ADVL1315), Cancer 124 (2018) 4548–4555, https://doi.org/10.1002/cncr.31725.

[42] J. Coventon, A review of the mechanism of action and clinical applications of sorafenib in advanced osteosarcoma, Journal of bone oncology 8 (2017) 4–7, https://doi.org/10.1016/j.jbo.2017.07.001.

[43] G. Grignani, E. Palmerini, P. Dileo, S.D. Asaftei, L. D'Ambrosio, Y. Pignochino, M. Mercuri, P. Picci, F. Fagioli, P.G. Casali, S. Ferrari, M. Aglietta, A phase II trial of sorafenib in relapsed and unresectable high-grade osteosarcoma after failure of standard multimodal therapy: an Italian Sarcoma Group study, Annals of oncology : official journal of the European Society for Medical Oncology 23 (2) (2012) 508–516.

[44] Q. Shi, Y.G. Chen, Interplay between TGF-β signaling and receptor tyrosine kinases in tumor development, Sci. China Life Sci. 60 (2017) 1133–1141, https://doi.org/10.1007/s11427-017-9173-5.

[45] N. Ungerleider, C. Han, J. Zhang, L. Yao, T. Wu, TGFβ signaling confers sorafenib resistance via induction of multiple RTKs in hepatocellular carcinoma cells, Mol. Carcinog. 56 (2017) 1302–1311, https://doi.org/10.1002/mc.22592.